Chemical Science

Accepted Manuscript

This article can be cited before page numbers have been issued, to do this please use: J. Tan, N. Yusuipujiang, J. Zhang, X. Jiang, Z. Zhang, Y. Wang and D. Ma, *Chem. Sci.*, 2026, DOI: 10.1039/D6SC01676F.

ROYAL SOCIETY OF CHEMISTRY

rsc.li/chemical-science

View Article Online
DOI: 10.1039/D6SC01676F

ARTICLE

Organocatalytic enantioselective synthesis and derivatizations of bridged *N,O*-acetal bicyclic scaffolds

Received 00th January 20xx,
Accepted 00th January 20xx

DOI: 10.1039/x0xx00000x

Jun Tan,[a†] Nasier Yusuipujiang,[a†] Jiyi Zhang,[a] Xin-Yi Jiang,[b] Zhihan Zhang,*[b] Yuji Wang,*[a] and Dengke Ma*[a]

The 7-oxa-2-azabicyclo[3.2.1]octane framework serves as a key structural motif in bioactive natural products, some of their natural sources were historically used in traditional remedies. Despite this significance, synthetic routes, particularly enantioselective ones, remain highly underdeveloped, limiting broader pharmaceutical exploration. To address this issue, we report a novel organocatalyzed approach enabling highly diastereo- and enantioselective access to related 7-oxa-2-azabicyclo[3.2.1]oct-3-ene cores with modifiable C-C double bonds. This method exhibits broad functional group compatibility, efficiently generating diverse, multifunctional chiral bicyclic products. Successful chirality-preserving transformations into complex polycyclic and fused systems highlight the strategy's synthetic value for accessing drug-like scaffolds. Mechanistic investigations including DFT calculations provide valuable insight into the reaction pathway governing stereoselectivity control. This work significantly expands the accessible chemical space of chiral bicyclic *N,O*-acetals and establishes a reliable platform for synthesizing enantiopure bridged bicycles.

1. Introduction

It remains an ongoing mission for synthetic chemists to expand libraries of artificial compounds beyond natural sources in complexity and diversity,[1-5] thereby addressing growing industrial and daily-life demands. Among the existing developed methods and technical approaches, organocatalytic cascade reactions possess unique advantages and significant applications, efficiently enabling the orchestrated formation of multiple chemical bonds in a single step. This allows chemists, by leveraging diverse known reactivities and combining ingenious substrate design and reaction planning, to facilitate rapid access to structurally complex natural products and biologically active molecules.[6-7]

For instance, 7-oxa-2-azabicyclo[3.2.1]octane scaffolds are core structural units in many natural products,[8-19] some of which adhered with remarkable biological activities, such as guiwuline,[12] acotarine B, acotarine E,[13] SB-219383,[14-15] and so on (Figure 1a). Notably, certain natural sources have even been used as traditional medicine for a long time.[12-13,16-19] However, methods for the enantioselective construction of such structures are rather rare. This methodological gap has constrained its broader application, especially within pharmaceutical contexts. With our continuous research interest on reaction discovery and organocatalysis, we hypothesized that starting from γ-hydroxy enal,[20] a simple and readily available compound integrated with alcohol and enal functionalities, would be a potential solution to synthesize bridged bicyclic *N,O*-acetals enabled by asymmetric iminium catalysis.[21-39] The idea is to utilize a nitrogen containing binucleophilic reagent and the ingeniously introduced γ-hydroxyl group on enal to undergo a highly regio- and stereoselective yet challenging cascade conjugate addition/cyclization to yield the expected bridged bicyclic compounds containing a *N,O*-acetal motif. Notably, this single-step reaction design forges three bonds consecutively (Figure 1b), which exhibits a synthetically ambitious endeavor requiring precise orchestration of the stereoselectivity control model and reactants' reactivity to suppress competing pathways (Figure 1c).[20,40-41]

Actually, by employing a simple unit integration strategy, we have discovered that γ-hydroxy enals/enones can indeed enable a series of novel transformations that differ significantly from those of conventional enal/enone frameworks. These include the neighboring group effect-driven synthesis of polyfunctionalized 5-alkenyl-3-furanones,[20] the selective construction of a racemic 2,7-dioxabicyclo[3.2.1]octane scaffold using HCl as a bifunctional catalyst through *in situ* generated 2,5-dihydrofuran-2-ol intermediate from γ-hydroxy enones and phenols, which differs a lot mechanistically from this work and the enantioselectivity control remains challenging.[42]

Opportunities and challenges go hand in hand, herein, we'd like to report an advance to the highly diastereo- and enantioselective synthesis of 7-oxa-2-azabicyclo[3.2.1]oct-3-enes from γ-hydroxy enal and 3-aminoacrylate via organocatalysis. Notable features include: (a) Enrich the molecule diversity and tool box for chemists and

[a] School of Pharmaceutical Sciences, Capital Medical University, Beijing 100069, China. Email: wangyuji@ccmu.edu.cn, madk@ccmu.edu.cn
[b] College of Chemistry, Central China Normal University, 152 Luoyu Road, Wuhan 430079, China. E-mail:zhihanzhang@ccnu.edu.cn
† These authors contribute equally.
Supplementary Information available: [details of any supplementary information available should be included here]. See DOI: 10.1039/x0xx00000x

View Article Online DOI: 10.1039/D6SC01676B

pharmaceutical scientists. (b) Enhanced pharmaceutical potential leveraging the inherent bioactivity of bicyclo[3.2.1]octane cores[43-45] and *N,O*-acetal motifs.[46-50] (c) Olefin functionality handles enabling downstream functionalization. (d) Transformable *N,O*-acetal moieties facilitating access to novel polycyclic and fused systems, enriching the synthetic potential of *N,O*-acetals. (e) Broad substrate scope with high efficiency. (f) Green reaction profile with water as the byproduct (Figure 1d).

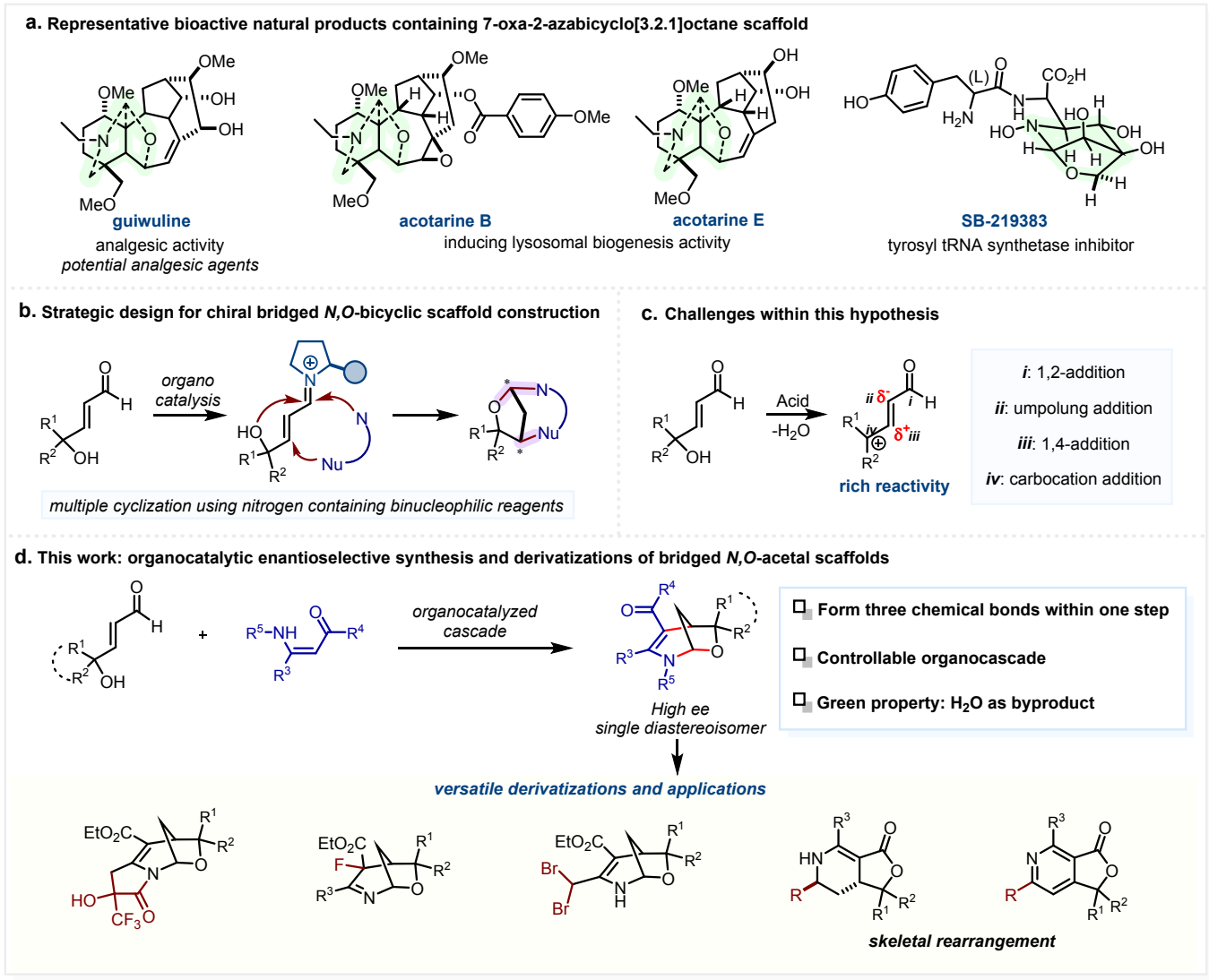

Figure 1. Organocatalytic enantioselective synthesis of 7-oxa-2-azabicyclo[3.2.1]oct-3-enes and diverse derivatizations.

2. Results and Discussion

2.1 Reaction optimization

Initial reaction screening employed γ-hydroxy enal **1a** and ethyl (*Z*)-3-aminobut-2-enoate **2a** with 20 mol% chiral aminocatalyst **A** and 30 mol% TFA in DCM at 45°C. Gladly, the desired product **3aa** contains 7-oxa-2-azabicyclo[3.2.1]oct-3-ene scaffold was successfully obtained in 51% yield with 83% ee (Table 1, entry 1).[53] Following catalyst screening of other chiral amine catalysts revealed **A** as optimal (For detailed optimizations, see Table S1 in the supporting information), while catalysts **B**[54] and **C** afforded obviously lower enantioselectivity (Table 1, entries 2-3). Subsequent evaluation of Brønsted acids (HCl, trichloroacetic acid, TfOH, TsOH·H_2O) identified TsOH·H_2O as superior, enhancing ee to 85% (Table 1, entry 4). Solvent optimization (DCE, $CHCl_3$, CCl_4, PhCl, toluene, EtOAc, MeCN) demonstrated MeCN's advantage taking both efficiency and enantioselectivity into consideration, delivering 68% yield and 90% ee (Table 1, entry 5).

Further refinement established better outcome with 25 mol% **A** in MeCN: complete conversion within 24 h afforded **3aa** in 78% yield and 93% ee (Table 1, entry 6). Notably, control experiment suggested a possible background reaction enabled by the TsOH·H_2O to form racemic **3aa** in 32% yield (Table 1, entry 7). Other control experiments demonstrated that no **3aa** formation without the acid or both catalyst **A** and TsOH·H_2O (Table 1, entries 8-9). Finally, a fine tuning of the TsOH·H_2O amount to 25 mol% was proved to be the best, yielding **3aa** in 81% yield and 93% ee (Table 1, entry 10).

View Article Online
DOI: 10.1039/D5SC01676F

Table 1. Reaction optimization.[a]

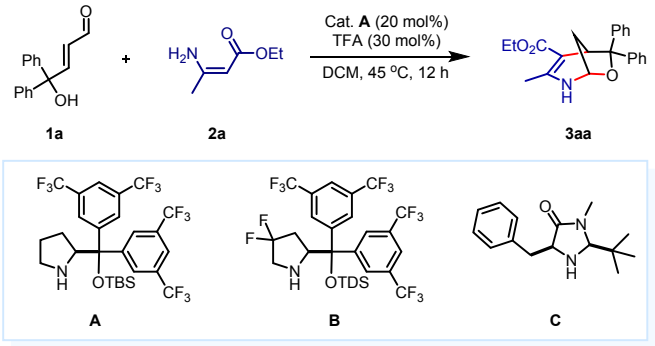

Entry	*Variation*	Conv. (%)	Yield (%)	Ee (%)
1	none	100	51	83
2	**B**	100	27	4
3	**C**	100	41	31
4	TsOH·H_2O	100	47	85
5	TsOH·H_2O/CH_3CN	100	68	90
6	**A** (25 mol%)/TsOH·H_2O/CH_3CN	100	78	93
7	NO **A** based on entry 6	87	32	0
8	NO TsOH·H_2O based on entry 6	31	0	-
9	NO **A** and TsOH·H_2O based on entry 6	13	0	-
10	**A** and TsOH·H_2O (25 mol%)/CH_3CN	100	81	93

[a] Reaction conditions: (*E*)-4-hydroxy-4,4-diphenylbut-2-enal **1a** (0.2 mmol), ethyl (*Z*)-3-aminobut-2-enoate **2a** (0.4 mmol), catalyst (0.04 mmol) and TFA (0.06 mmol) were stirred in DCM (2 mL) at 45 °C for 12 h. Conversion and yield were determined by NMR using mesitylene as the internal standard. The ee values were determined by HPLC using a chiral stationary phase.

2.2 Scope of the reaction

Having established the best conditions for the preparation of 7-oxa-2-azabicyclo[3.2.1]oct-3-ene scaffolds, we next started the substrate scope studies (Figure 2). Apart from the template product **3aa** formed in 79% yield with 93% ee, its enantiomer *ent*-**3aa** could be obtained in 74% yield with -94% ee in the presence of *ent*-**A**, providing a reliable access for both configurations of 7-oxa-2-azabicyclo[3.2.1]oct-3-ene scaffolds. In addition, the γ-substituents could be varied in a broad scope, including phenyls substituted with electron withdrawing 4-fluoride (**3ba**), 4-chloride (**3ca**), 4-bromide (**3da**),[55] 3-chloride (**3ea**), and electron donating 4-methyl (**3fa**), 4-methoxy (**3ga**), to afford the corresponding products in 69-80% yield with 94-95% ee, as well as 2-naphthyl (**3ha**) in 72% yield with 92% ee, 9-fluorenylidene (**3ia**) in 67% yield with 93% ee, and 5*H*-dibenzo[*a*,*d*][7]annulen-5-ylidene (**3ja**) in 84% yield and 90% ee. Besides, the structure and absolute configuration of **3ja** was further confirmed by X-ray single crystal diffraction study.

What's more, the γ-position could be alkyl groups as well, such as methyl (**3ka**), benzyl (**3la**), and 1,4-butanediyl (**3ma**), to give the products in 58-71% yield with 88-94% ee. Interestingly, the structures of **3ia**, **3ja**, and **3ma** also contain a spirocyclic moiety beyond the 7-oxa-2-azabicyclo[3.2.1]oct-3-ene scaffold. When R^1 and R^2 at the γ-position are both hydrogens, the desired product **3na** was obtained in moderate yield with 95% ee. Notably, the 2-oxa-8-azabicyclo[3.3.1]non-6-ene scaffold **3oa** could also be synthesized from δ-hydroxy enal in high yield with 88% ee. While if R^1 and R^2 are different, for example one is phenyl and the other is methyl, **3pa** was formed with 1:1 dr.

For the 3-aminoacrylates, the ester part could be changed to methyl (**3ab**), isopropyl (**3ac**), benzyl (**3ad**), and (*E*)-3-phenylprop-2-en-1-yl (**3ae**), affording 52-78% yield with 91-95% ee. Meanwhile, the R^3 group could be varied to ethyl, phenyl, 2-thienyl, and 2-furanyl to deliver **3af** to **3ai** in moderate to good yield with 86-95% ee. Then *N*-methyl substituted 3-aminoacrylate also took part in the reaction smoothly to generate **3aj** in 59% yield with 91% ee under aminocatalyst **A2**. The application of this transformation could further be highlighted by the tolerate of sitagliptin (a therapeutic drug for diabetes) derived 3-aminoacrylate to give **3ak** in good enantioselectivity. Starting from (*E*)-4-hydroxybut-2-enal, the corresponding products **3ne** and **3nl** were formed smoothly with good enantioselectivity by changing the ester moiety to (*E*)-3-phenylprop-2-en-1-yl and cyanoethyl, respectively.

2.3 Synthetic potentials and applications

The developed strategy could be applied to the gram scale synthesis of **3aa** with maintained high enantioselectivity (Figure 3a). Simultaneously, thanks to the *N,O*-acetal moiety and olefin functionality, the target 7-oxa-2-azabicyclo[3.2.1]oct-3-ene products bring versatile derivatizations to afford synthetically useful chiral polycyclic and fused systems that otherwise couldn't be easily accessed (Figure 3a). For instance, trifluoromethyl containing polycyclic compound **5** and **5'** were obtained in 74% yield and ~1.1:1 dr with 95% ee and 93% ee, respectively, by the reaction of **3aa** with methyl 3,3,3-trifluoropyruvate. The structure and absolute configuration of **5'** was also confirmed by X-ray single crystal diffraction study.

Fluoride containing compound **6** could be formed in 78% yield with 95% ee by the simple treatment of **3aa** with Selectfluor. Notably, introducing fluoride and fluoride containing groups into the bridged bicyclic compounds would help to improve the pharmacokinetic and molecule anti-oxidative properties, thus bring enhanced bioactivities.[56] Next, the reaction of **3aa** with NBS (2.2 equiv.) afforded dibromomethylated product **7** in 66% yield with 95% ee as well. It is of interest that bridged bicyclic **3aa** could be transferred to fused compound **8** through skeletal rearrangement in the presence of $LiAlH_4$ with full enantioselectivity retention.

Herein, $LiAlH_4$ might firstly act as a base to remove the proton on nitrogen to form nitrogen anion intermediate **Int-A**, then the *N,O*-acetal decomposed to yield **Int-B**, followed by lactonization via intramolecular transesterification to generate **Int-C**. Ultimately, nucleophilic hydride 1,2-addition to imine would afford **8** contain 5,6,7,7*a*-tetrahydrofuro[3,4-*c*]pyridin-3(1*H*)-one scaffolds (Figure 3b). Inspired by this skeletal rearrangement strategy, compound **9** was formed in 61% yield with 96% ee from **3aa** in the presence of NaOH and indole nucleophile. It is the nitrogen attack the imine in this case based on structural analysis. Remarkably, compound **10** could be formed in 96% yield with 95% ee from the reaction of **3aa** and PhMgBr, with the Grignard reagent acting as both base and nucleophile. The structure and absolute configuration of **10** is also confirmed by X-ray single crystal diffraction study.

View Article Online
DOI: 10.1039/D6SC01676F

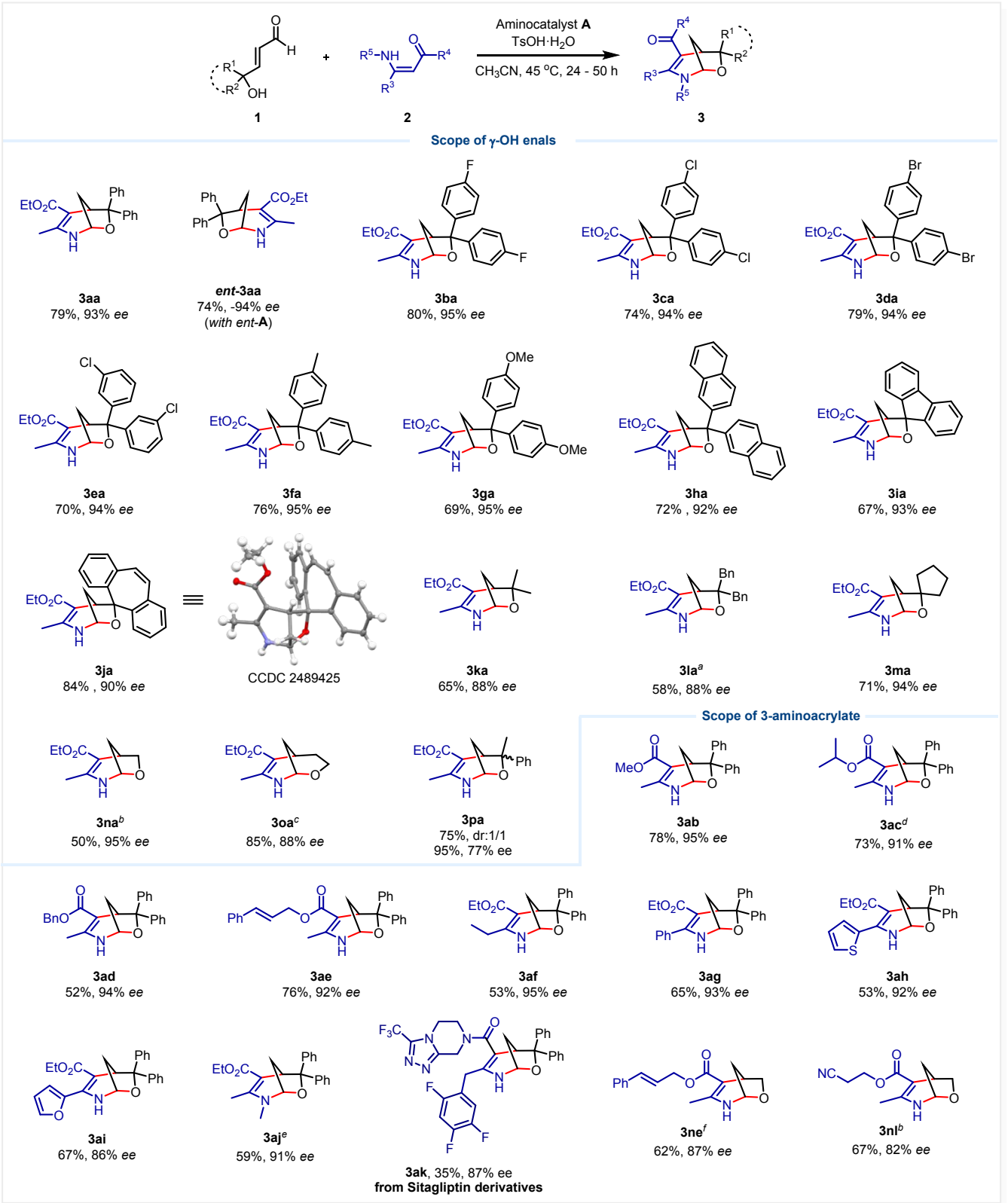

Figure 2. Substrate Scope. Reaction conditions: **1** (0.4 mmol), **2** (0.8 mmol), aminocatalyst (0.1 mmol) and TsOH·H_2O (0.1 mmol) were stirred in ACN (4 mL) at 45 °C for 24 - 50 h. The ee values were determined by HPLC using a chiral stationary phase. The dr values were determined by ^{1}H NMR. [a]**A2** (0.12 mmol) and TsOH·H_2O (0.12 mmol), rt. [b]Rt without acid. [c]**A** (0.12 mmol) and TsOH·H_2O (0.12 mmol), 10 °C. [d]65 °C. [e]**A2** (0.12 mmol) and TsOH·H_2O (0.12 mmol). [f]**A** (0.12 mmol) and TsOH·H_2O (0.12 mmol), rt.

View Article Online
DOI: 10.1039/D6SC01676F

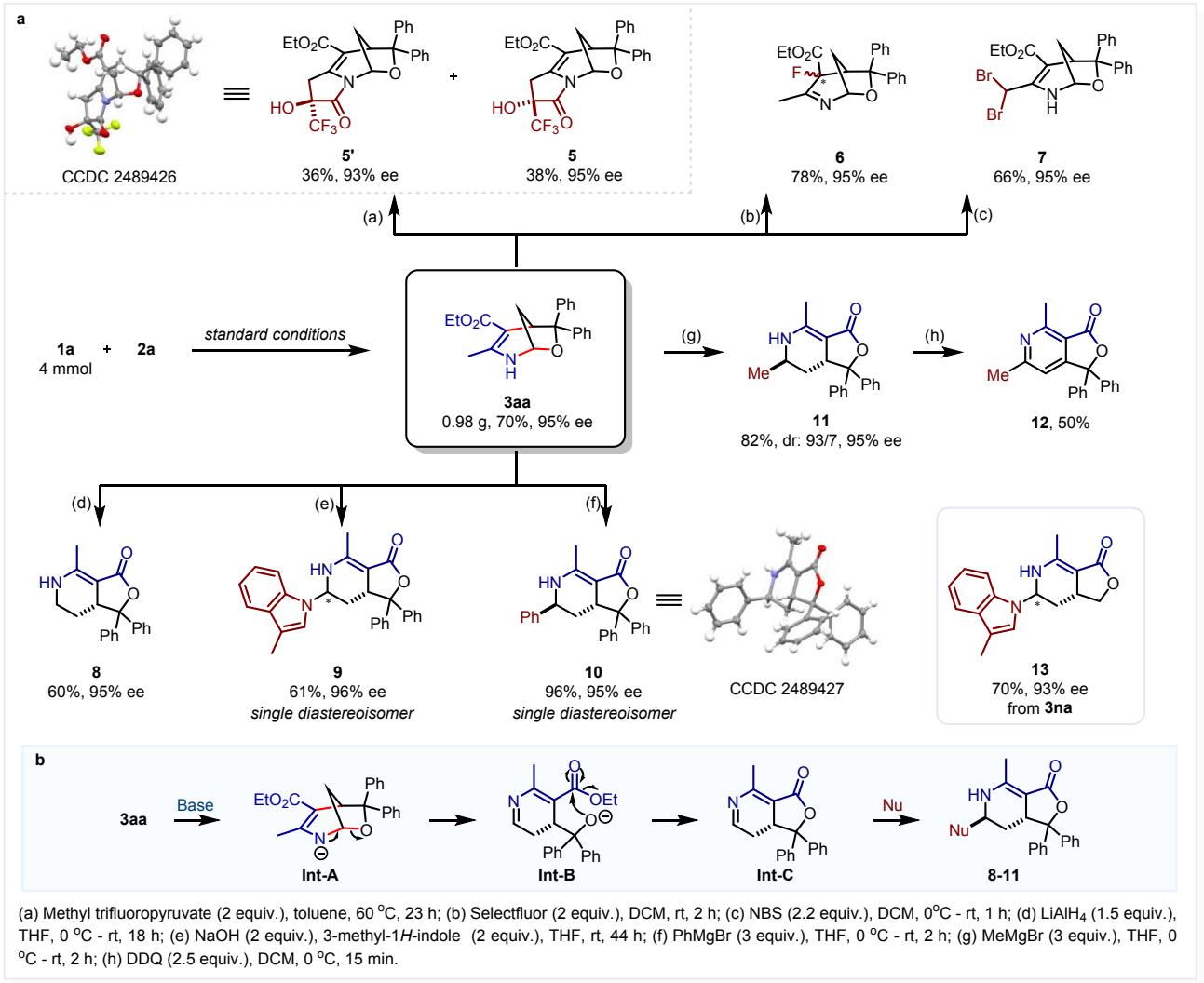

Figure 3. Synthetic potentials. a, Gram-scale reaction and transformation to 5,6,7,7*a*-tetrahydrofuro[3,4-*c*]pyridin-3(1*H*)-ones as well as other applicable structures. b, Plausible pathway for the formation of **8**-**11** from **3aa**.

When CH_3MgBr was used, corresponding product **11** was obtained in 82% yield and 93:7 dr with 95% ee. And the tetrahydropyridine ring in **11** could further be oxidized to aromatic pyridine **12** using DDQ. Reaction of **3na** with 3-methylindole also afforded **13** in 70% yield and 93% ee.

2.4 Mechanistic studies

To elucidate the mechanism of this reaction, detailed mechanistic studies were undertaken. Initially, the template reaction at room temperature yielded **3aa** in 47% yield with 96% ee, along with a byproduct **14** (15% yield, 98% ee). Notably, compound **14** could be converted to the product **3aa** under the standard conditions in 80% yield (>99% ee), concomitantly generating **2a** in 61% yield (Figure 4a, condition A). The release of **2a** from **14** was shown to be independent of the aminocatalyst, as **3aa** formation proceeded with nearly identical results using only 25 mol% $TsOH{\cdot}H_2O$ (Figure 4a, condition B). In contrast, the reaction conducted in the absence of both aminocatalyst and $TsOH{\cdot}H_2O$ afforded **3aa** in only 25% yield and **2a** in 21% yield, with 54% of compound **14** recovered (Figure 4a, condition C). These findings strongly suggest that compound **14** likely acts as an intermediate and that the acid $TsOH{\cdot}H_2O$ is responsible for its transformation to the final product **3aa**. Further evidence from the reaction monitoring also supported the intermediacy of **14**.

Next, although the *N*-methyl substituted substrate ultimately afforded product **3aj** in satisfactory yield and enantioselectivity after simple optimization, the *N*-substituents on the 3-aminoacrylates exerted a significant influence on both the yield and enantioselectivity. For example, under the standard conditions: *N*-unsubstituted ethyl (*Z*)-3-aminobut-2-enoate (**2a**) afforded **3aa** in 79% yield with 93% ee; *N*-methyl substituted ethyl (*Z*)-3-(methylamino)but-2-enoate (**2j**) afforded **3aj** in 68% yield with a significantly lower ee of 58%; *N*-benzyl substituted ethyl (*Z*)-3-(benzylamino)but-2-enoate (**2l**) afforded **3al** in only 46% yield with 24% ee (Figure 4b). These results demonstrate the pronounced impact of steric hindrance on both reactivity and enantioselectivity.

View Article Online
DOI: 10.1039/D6SC01676F

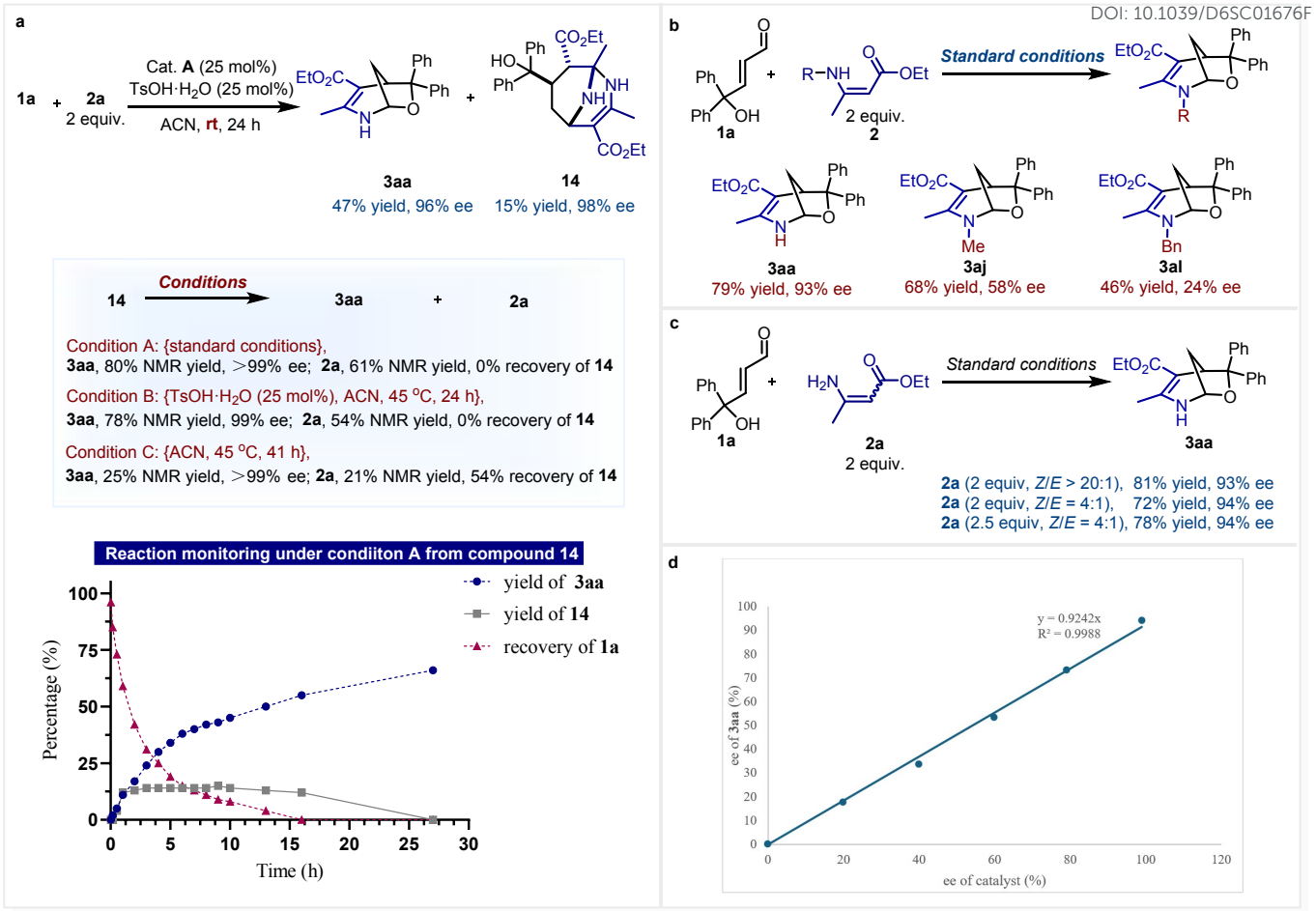

Figure 4. Mechanistic studies. a, Characterization of possible intermediate. b, Effect of *N*-substitution on the 3-aminoacrylate: yield and ee. c, Effect of *Z*/*E* configuration on the 3-aminoacrylate: yield and ee. d, Non-linear effect study.

Furthermore, the geometry of the double bond in the 3-aminoacrylates also significantly affected the reaction yield. As shown, the reaction utilizing predominantly the *Z*-isomer **2a** (*Z*/*E* > 20:1) afforded **3aa** in 81% yield with 93% ee. In contrast, employing a mixture of **2a** (*Z*/*E* = 4:1) afforded **3aa** in a lower yield of 72% (94% ee). Increasing the loading of this *Z*/*E* mixture (4:1) to 2.5 equivalents improved the yield of **3aa** to 78% while maintaining the same enantioselectivity (94% ee) (Figure 4c). These results suggest a difference in reactivity between the *Z*- and *E*-configured olefins in the transition state. A study of the nonlinear effect revealed a clear linear correlation between the ee of the product and that of the catalyst. This linear relationship demonstrates that only one chiral aminocatalyst molecule is involved in the enantioselectivity-control step (Figure 4d).

Based on the mechanistic investigations, a preliminarily plausible reaction mechanism was proposed (Figure 5). The chiral iminium intermediate **Int-D** forms from γ-hydroxy enal **1a** and the aminocatalyst. Subsequently, **2a** undergoes a stereoselective nucleophilic 1,4-addition to **Int-D**, affording intermediate **Int-E**. Within this step, the *Z*-configured isomer of **2a** likely exhibits higher reactivity than its *E*-counterpart, potentially due to an intramolecular hydrogen-bonding interaction.[57] Intermediate **Int-E** then diverges along two possible pathways: (i) Hydrolysis of **Int-E** yields **Int-F**, which goes through consecutively intramolecular cyclization to afford bridged bicyclic product **3aa** ensured by the γ-OH and the NH_2 moiety in the 3-aminoacrylate (Figure 5, Path A).[58] (ii) A second molecule of **2a** undergoes 1,2-addition to the imine moiety in **Int-E**, leading to the formation of **Int-G**. Hydrolysis of **Int-G** then affords **Int-H**. Subsequently, intramolecular condensation generates **Int-I**, with elimination of one water assisted by the acid. Then there are two competing pathways exist. As compound **14** is observed in the reaction, it can be explained by the cyclization from another molecule of 3-aminoacrylate via **Int-I**, followed by imine-enamine isomerization (**Int-J**). The other possibility involves the direct intramolecular attack of the γ-OH to the imine within **Int-I** to afford **Int-K**, accompanied with the elimination of one molecule of **2a**. Final isomerization would yield product **3aa**. Notably, the conversion between **Int-I**/**Int-J** and compound **14** should be reversible as **14** could be transferred to **3aa** in the presence of acid as proved by mechanistic studies in Figure 4a (Figure 5, Path B).

View Article Online
DOI: 10.1039/D6SC01676F

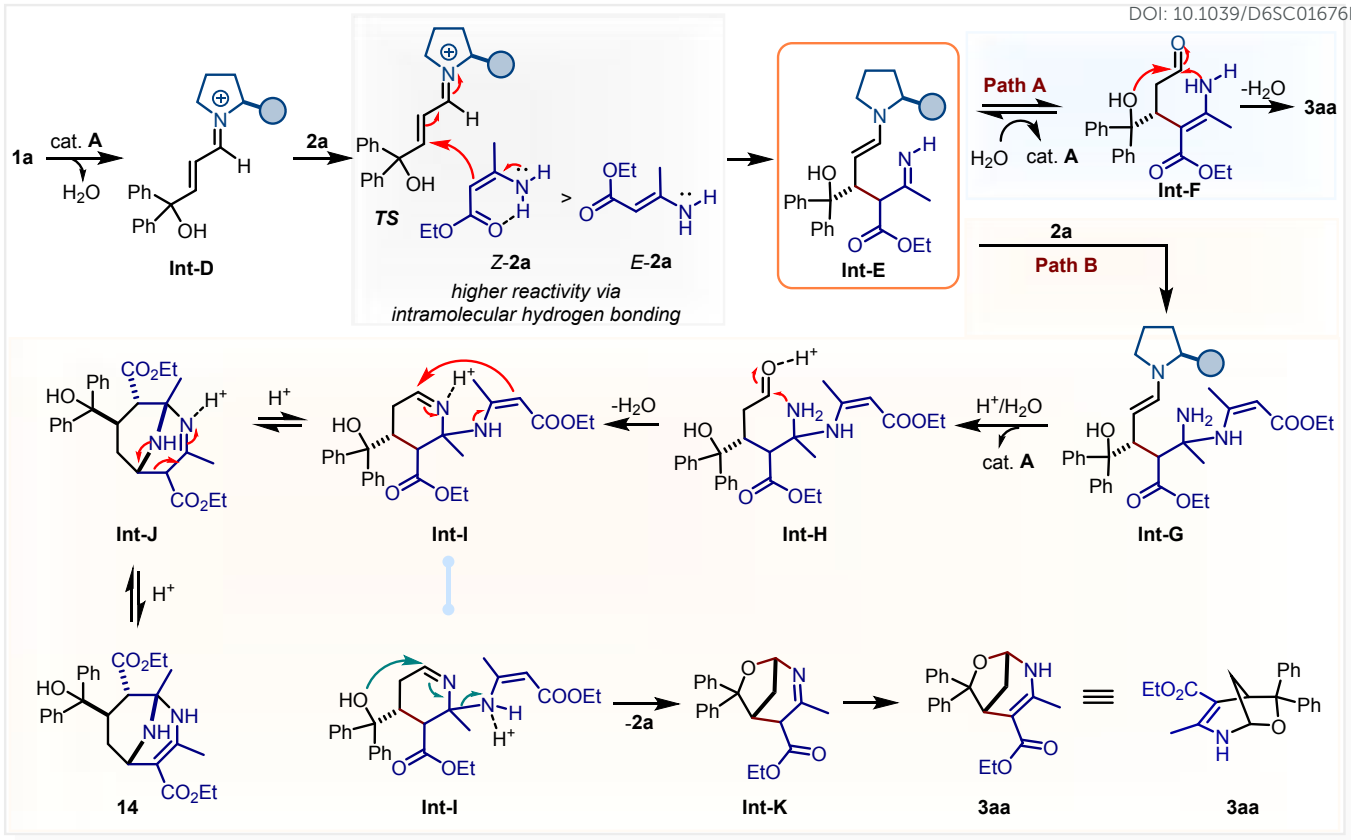

Figure 5. Plausible mechanism.

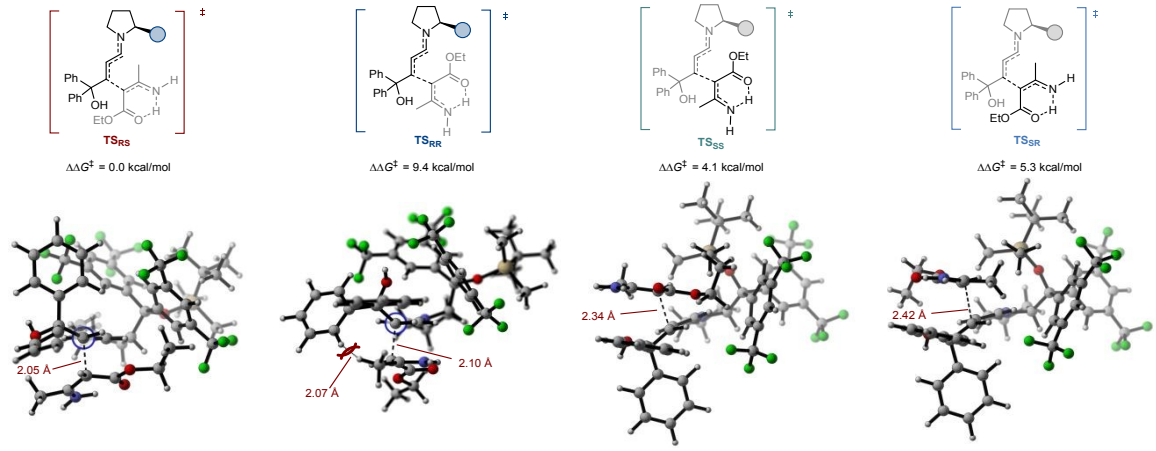

Figure 6. DFT calculations on the stereo-determining transition states.

Further density functional theory (DFT) calculations were conducted on the nucleophilic attack steps (Figure 6). Our calculations show that the **2a** is more stable with the intramolecular hydrogen bond and this trend is preserved in transition state (see Figure S6 in the supporting information), which is consistent with the experimental observations that *Z*/*E* ratio of **2a** does not affect the stereoselectivity. Herein our discussion is focused on the transition states with this intramolecular hydrogen bond retained. As shown in Figure 6, compared with the most favorable transition state **TS_{RS}**, in both **TS_{SS}** and **TS_{SR}**, **2a** approaches β-carbon of **Int-D** from the upper side which is congested due to the steric of catalyst, evidenced by elongated C–C bond length (larger than 2.34 Å). Further distortion/interaction analysis identified significantly weaker interaction energies between catalyst and **2a**. On the other hand, in **TS_{RR}**, the steric from the methyl group of **2a** enforces the distortion of the C=C double bond of eniminium ion intermediate with a smaller Wiberg bond index (WBI) of 1.603 (see from the Newman projection). This distortion does not occur in **TS_{RS}** since the methyl group oriented to empty space, and the corresponding C=C double bond has stronger WBI of 1.626. These results are consistent with the observed enantioselectivity and X-ray analysis of the products.

Conclusions

In conclusion, an innovative and efficient organocatalytic strategy has been developed for the highly diastereo- and enantioselective synthesis of 7-oxa-2-azabicyclo[3.2.1]oct-3-ene scaffolds. This reaction demonstrates good functional group tolerance, providing access to a series of multifunctional chiral bridged bicyclic compounds. These products feature modifiable *N,O*-acetals, C-C double bonds, and carboxylic acid derivatives, offering enhanced potential for facile modification. Detailed mechanistic studies provide valuable understanding of the complex pathway involving concurrent formation of three bonds in a single step. Further DFT calculations disclosed the origination and control of enantioselectivity within the conjugate addition step. Subsequent synthetic transformations and skeletal rearrangement to diverse polycyclic and fused ring systems with complete chirality transfer underscore the method's potential utility in organic synthesis and drug discovery. This approach not only enriches the molecular diversity of chiral bridged bicyclic *N,O*-acetals but also establishes a robust platform for preparing optically active bridged bicyclic compounds. Research applying this strategy to construct further chiral bridged bicyclic compounds is currently underway in our laboratory.

Author contributions

D.M. designed the project and directed the work. J.T. and N.Y. developed the reaction, investigated the substrate scope and studied the reaction mechanism. Y.W. directed the bioactivity test work. J.Z. investigated the anti-proliferative activity studies. X.J. performed the DFT calculations under the guidance of Z.Z. All authors contributed to the experimental design and the interpretation of data. J.T., Z.Z., Y.W., and D.M. wrote the paper with input from all authors.

Conflicts of interest

There are no conflicts to declare.

Data availability

All relevant data supporting the findings are included in the Article and its Supplementary Information or are available from the corresponding authors upon reasonable request.

Acknowledgements

Financial support from National Natural Science Foundation of China (Grant No. 22201187), and the starting grant from Capital Medical University (Grant No. 3100-12500121 and 3100-12600118) are gratefully acknowledged. The authors thanks for the assistance provided by the analytical testing center of Capital Medical University.

Notes and references

View Article Online
DOI: 10.1039/D6SC01676F

1 K. C. Nicolaou, C. R. H. Hale, C. Nilewski and H. A. Ioannidou, *Chem. Soc. Rev.,* 2012, **41**, 5185–5238.
2 L. Yang, K. L. Chan, K. K. Cheung, P. Chiu, Z. Lin and J. Sun, *Nat. Synth.,* 2025, **4**, 1223–1231.
3 S. Caille, S. Cui, M. M. Faul, S. M. Mennen, J. S. Tedrow and S. D. Walker, *J. Org. Chem.,* 2019, **84**, 4583–4603.
4 B. A. Wright and R. Sarpong, *Nat. Rev. Chem.,* 2024, **8**, 776–792.
5 L. Min, Y.-J. Hu, J.-H. Fan, W. Zhang and C.-C. Li, *Chem. Soc. Rev.,* 2020, **49**, 7015–7043.
6 C. Grondal, M. Jeanty and D. Enders, *Nat. Chem.,* 2010, **2**, 167–178.
7 P. Bonilla, Y. P. Rey, C. M. Holden and P. Melchiorre, *Angew. Chem. Int. Ed.,* 2018, **57**, 12819–12823.
8 F.-P. Wang, Z.-B. Li, X.-P. Dai and C.-S. Peng, *Phytochemistry,* 1997, **45**, 1539–1542.
9 D.-L. Chen, L.-Y. Lin, Q.-H. Chen, X.-X. Jian and F.-P. Wang, *J. Asian Nat. Prod. Res.,* 2003, **5**, 209–213.
10 P. Tang, D. L. Chen, X. X. Jian and F. P. Wang, *Chin. Chem. Lett.,* 2007, **18**, 704–707.
11 W. Xu, L. Shan, S. Huang, S. Li and X. Zhou, *Chin. J. Org. Chem.,* 2016, **36**, 2739–2742.
12 D.-P. Wang, H.-Y. Lou, L. Huang, X.-J. Hao, G.-Y. Liang, Z.-C. Yang and W.-D. Pan, *Bioorg. Med. Chem. Lett.,* 2012, **22**, 4444–4446.
13 Y. Si, X. Ding, T. A. Adelakuna, Y. Zhang and X.-J. Hao, *Fitoterapia,* 2020, **147**, 104738.
14 A. L. Stefanska, N. J. Coates, L. M. Mensah, A. J. Pope, S. J. Ready and S. R. Warr, *J. Antibiot.,* 2000, **53**, 345–350.
15 C. S. V. Houge-Frydrych, S. A. Readshaw and D. J. Bell, *J. Antibiot.,* 2000, **53**, 351–356.
16 T.-P. Yin, L. Cai, Y. Xing, J. Yu, X.-J. Li, R.-F. Mei and Z.-T. Ding, *J. Asian Nat. Prod. Res.,* 2016, **18**, 603–610.
17 R. Guo, C. Guo, D. He, D. Zhao and Y. Shen, *Chin. J. Chem.,* 2017, **35**, 1644–1647.
18 T. Yin, Y. Shu, R. Mei, J. Wang, L. Cai and Z. Ding, *Biochem. Syst. Ecol.,* 2018, **81**, 99–101.
19 Z. Lv, L. Gao, C. Cheng, W. Niu, J.-L. Wang and L. Xu, *Chem. Asian J.,* 2018, **13**, 955–958.
20 J. Tan, C. Xie, Y. Qiu and D. Ma, *Chin. J. Chem.,* 2025, **43**, 1643–1650.
21 A. Erkkilä, I. Majander and P. M. Pihko, *Chem. Rev.,* 2007, **107**, 5416–5470.
22 D. W. C. MacMillan, *Nature,* 2008, **455**, 304–308.
23 G. Bartoli and P. Melchiorre, *Synlett*, 2008, **12**, 1759–1772.
24 S.-H. Xiang and B. Tan, *Nat. Commun.,* 2020, **11**, 3786.
25 Z.-C. Chen, W. Du and Y.-C. Chen, *Chin. J. Chem.,* 2021, **39**, 1775–1786.
26 G. Zhan, W. Du and Y.-C. Chen, *Chem. Soc. Rev.,* 2017, **46**, 1675–1692.
27 Y. Gu, Y. Wang, T.-Y. Yu, Y.-M. Liang and P.-F. Xu, *Angew. Chem. Int. Ed.,* 2014, **53**, 14128–14131.
28 A. Noole, M. Borissova, M. Lopp and T. Kanger, *J. Org. Chem.,* 2011, **76**, 1538–1545.
29 G. Bergonzini and P. Melchiorre, *Angew. Chem. Int. Ed.,* 2012, **51**, 971–974.
30 X. Jiang, B. Tan and C. F. Barbas III, *Angew. Chem. Int. Ed.,* 2013, **52**, 9261–9265.
31 G. Luo, Z. Huang, S. Zhuo, C. Mou, J. Wu, Z. Jin and Y. R. Chi, *Angew. Chem. Int. Ed.,* 2019, **58**, 17189–17193.
32 S. Hu, J. Wang, G. Huang, K. Zhu and F. Chen, *J. Org. Chem.,* 2020, **85**, 4011−4018.
33 K. Daskalakis, N. Umekubo, S. Indu, G. Kawauchi, T. Taniguchi, K. Monde and Y. Hayashi, *Angew. Chem. Int. Ed.,* 2025, **64**, e202500378.

View Article Online
DOI: 10.1039/D6SC01676F

34 F. Wu, Q. Peng, Y.-J. Li, Y. Xiao and J.-J. Feng, *Chin. J. Chem.,* 2026, **44**, 241–250.
35 S. Brandau, A. Landa, J. Franzén, M. Marigo and K. A. Jørgensen, *Angew. Chem. Int. Ed.*, 2006, **45**, 4305–4309.
36 A. Carlone, S. Cabrera, M. Marigo and K. A. Jørgensen, *Angew. Chem. Int. Ed.*, 2007, **46**, 1101–1104.
37 S. Cabrera, J. Alemán, P. Bolze, S. Bertelsen and K. A. Jørgensen, *Angew. Chem. Int. Ed.*, 2008, **47**, 121–125.
38 E. Reyes, H. Jiang, A. Milelli, P. Elsner, R. G. Hazell and K. A. Jørgensen, *Angew. Chem. Int. Ed.*, 2007, **46**, 9202–9205.
39 G. Dickmeiss, K. L. Jensen, D. Worgull, P. T. Franke and K. A. Jørgensen, *Angew. Chem. Int. Ed.*, 2011, **50**, 1580–1583.
40 J. Tan, C. Xie, N. Yusuipujiang, M. Xu, L. Wang and D. Ma, *J. Org. Chem.,* 2025, **90**, 8687−8692.
41 T. Lei, J. Tan, Y. Zhang and D. Ma, *Org. Biomol. Chem.,* 2025, **23**, 8170–8175.
42 C. Xie, J. Tan, J. Zhang, Y. Zhang, Y. Wang and D. Ma, *Chin. J. Chem*., 2026, **44**, 1419–1425.
43 M.-H. Filippini and J. Rodriguez, *Chem. Rev.,* 1999, **99**, 27–76.
44 M. Presset, Y. Coquerel and J. Rodriguez, *Chem. Rev.,* 2013, **113**, 525–595.
45 K. Gao, J. Hu and H. Ding, *Acc. Chem. Res.,* 2021*,* **54**, 875−889.
46 R. A. Mosey and P. E. Floreancig, *Nat. Prod. Rep.,* 2012, **29**, 980–995.
47 R. H. Cichewicz, F. A. Valeriote and P. Crews, *Org. Lett.,* 2004, **6**, 1951–1954.
48 R. N. Enright, J. L. Grinde, L. I. Wurtz, M. S. Paeth, T. R. Wittman, E. R. Cliff, Y. T. Sankari, L. T. Henningsen, C. Tan, J. D. Scanlon and P. H. Willoughby, *Tetrahedron,* 2016, **72**, 6397–6408.
49 A. D. Kouvelas, M. G. Kallitsakis and I. N. Lykakis, *Chem. Eur. J.,* 2025, **31**, e202500413.
50 J. S. Novais, M. F. Carvalho, M. S. Ramundo, C. O. Beltrame, R. B. Geraldo, A. K. Jordão, V. F. Ferreira, H. C. Castro and A. M. S. Figueiredo, *Sci. Rep.,* 2020, **10**, 19631.
51 J. Sun, S. Wang, K. C. Harper, Y. Kawamata and P. S. Baran, *Nat. Chem.*, 2025, **17**, 44–53.
52 P. Oroz, C. Bretón, M. Torres, I. Olagaray, E. Sainz, C. M. Segovia, A. Avenoza, J. H. Busto, F. Corzana, G. Jiménez-Osés and J. M. Peregrina, *J. Org. Chem.*, 2025, **90**, 16238−16248.
53 Hantzsch ester byproduct **4aa** (14% yield) was formed alongside via aldehyde cyclization, for details, see Table S1. The possible mechanism for its formation is also proposed in the SI, see Fig. S4.
54 M. Silvi, C. Verrier, Y. P. Rey, L. Buzzetti and P. Melchiorre, *Nat. Chem.,* 2017, **9**, 868–873.
55 Initial screening revealed anti-proliferative properties against 4T1 cells in several compounds, with **3da** exhibiting an IC_{50} of 31.3 ± 7.2 μM. For details, see the anti-proliferative activity test part in the supporting information.
56 S. Baldon, L. Dell'Amico and S. Cuadros, *Eur. J. Org. Chem.,* 2024, **27**, e202400604.
57 X. Zhang, X. Lu, Y. Zou, J. Lang, Y. Wang and G. Zhao, *Org. Biomol. Chem.,* 2025, **23**, 4884–4887.
58 For a more detailed mechanism diagram, see Figure S3 in the SI.

View Article Online
DOI: 10.1039/D6SC01676F

The supporting data has been provided as part of the Supplementary information. Supplementary information: Tables S1, NMR spectra and further experimental details, see DOI: [URL – format https://doi.org/DOI]. Deposition numbers 2489425 (for **3ja**), 2489426 (for **5'**), and 2489427 (for **10**) contain the supplementary crystallographic data for this paper. These data are provided free of charge by the joint Cambridge Crystallographic Data Centre and Fachinformationszentrum Karlsruhe Access Structures service.